Indian Journal of Advances in Chemical Science

Article

In Silico Investigation of Charge Transfer and Non-covalent Interactions between Nitro-polycyclic Aromatic Hydrocarbons and DNA/RNA Bases and Base Pairs using Density Functional Theory

Mohmedyasin F. Mansuri[1], Shravan B. Rathod[2]*

[1]Department of Microbiology, Smt. S. M. Panchal Science College (Hemchandracharya North Gujarat University, Patan), Talod, North Gujarat, India, [2]Department of Chemistry, Smt. S. M. Panchal Science College (Hemchandracharya North Gujarat University, Patan), Talod, North Gujarat, India

ABSTRACT

The electrophilicity-based charge transfer (ECT) between nine nitro-polycyclic aromatic hydrocarbons (NPAHs) and seven DNA/RNA bases and base pairs was investigated and compared using ΔN and ECT methods at density functional theory level theory. The ground-state geometries of molecules were optimized at density hybrid functional B3LYP and Pople basis set 6-31 G*. ΔN and ECT methods predict different results for charge transfer, and ECT method has a considerably higher amount of charge transfer between two systems compared to ΔN method. Binding energies of NPAHs with Guanine-cytosine watson-crick (GCWC) and Adenine-thymine watson-crick (ATWC) base pairs were calculated and then corrected using B3LYP-gCP-D3/6-31G* scheme. The topological analysis of electron charge density was performed to investigate the non-covalent interactions between NPAHs and DNA/RNA bases and base pairs using atoms in molecules (AIM) approach.

Key words: Particulate matter$_{2.5}$, Carcinogenic, Toxins, Electrophilicity index, Binding energy.

1. INTRODUCTION

The emission of nitro-polycyclic aromatic hydrocarbons (NPAHs) into the environment is mainly due to incomplete combustion of coal from factories, vehicles, trucks, and electricity-generating stations. These emitted NPAHs are a part of atmospheric particulate matter ($PM_{2.5}$) having 2.5 μm or less diameter [1-2]. In addition to the presence of NPAHs in $PM_{2.5}$, they are also detected in river water of some regions of China in pg/mL level [3]. It is reported that polycyclic aromatic hydrocarbons (PAHs), oxygen-substituted PAHs, and the nitro group-containing PAHs (nitro-PAHs) are carcinogenic and have the mutagenic potential [4]. The evolution studies of excess cancer risk by inhalation of PAHs and NPAHs have also been reported [5-7].

The prediction of the relationship between chemical structure and its toxicity based on respective molecular structural parameters can be established by quantitative structure-activity relationship models [8]. In molecular systems, a number of non-covalent interactions between protein-protein, DNA-protein, drug-protein, and other various molecules occur through hydrogen [9-12], halogen [13-15], chalcogen [16-18], and pnictogen bonds [19-22]. Poater *et al*. [23] investigated the role of hydrogen bonding and π-π stacking interactions to stabilize the B-DNA structure. Researchers also have reported π-π stacking interactions between various molecular systems [24-29]. The DNA base-stacking interactions [30] and π-π stacking interactions between PAHs and nucleobases have been reported [31]. Fu *et al*. [32] experimentally reported that the derivatives of nitrobenzo[a]pyrene have drastically different DNA binding, mutagenicity, and metabolism pattern compared to their parent PAHs and the orientation of the nitro group plays an important role in these properties.

To determine the kind of interactions between the toxins and biological molecules, researchers have proposed some reactivity descriptors such as chemical potential (μ), chemical hardness (η), softness (S), and electrophilicity index (ω) [33-35]. Applying these descriptors, charge transfer methods, ΔN [34] and electrophilicity-based charge transfer (ECT) [36], have been developed to predict the interactions between the systems.

The toxicity of a different class of PAHs such as polychlorinated dibenzofurans, polyhalogenated dibenzo-p-dioxins, and polychlorinated biphenyls has been investigated using ΔN method [37,38]. Interactions among proteins, DNA, drugs, and ligands occur through covalent bonding, dative bonding, or hydrogen bonding by exchanging partial charge [35]. In the field of drug design, using these charge transfer descriptors, Rizwana *et al*. [39] have analyzed the activities and potencies of drug molecules for specific targets. Ash *et al*. [40] have detected the transition states and products of the proton transfer processes in molecules through these descriptors.

In the present work, B3LYP hybrid functional of density functional theory (DFT) with 6-31G* Gaussian basis set was used to calculate reactivity descriptors of selected NPAHs and DNA/RNA bases and base pairs.

For the comparison of ECT interactions between the two systems, ΔN and ECT methods were used. Furthermore, non-covalent interactions

***Corresponding author:**
E-mail: shravanathorizon93@gmail.com

ISSN NO: 2320-0898 (p); 2320-0928 (e)
DOI: 10.22607/IJACS.2019.703003

Received: 26th July 2019;
Revised: 08th August 2019;
Accepted: 12th August 2019

and binding affinity of some NPAHs with ATWC and GCWC base pairs were studied. The chemical structures of nine NPAHs and seven DNA/RNA bases and base pairs are shown in Figure 1.

2. THEORY AND COMPUTATIONAL DETAILS

2.1. Theory

The chemical potential (μ) and chemical hardness (η) were defined by Parr and Pearson, in 1983 [34]. A chemical potential (Equation 1) is a form of the amount of energy changes with respect to electron number (N) of the molecule at a certain external potential which is generated by nuclei of the molecular system;

$$\mu = \left(\frac{\partial E}{\partial N}\right)_{V(\vec{r})} \quad (1)$$

While chemical hardness (Equation 2) is a variation of chemical potential (μ) with respect to the electron number of molecular systems at fixed external potential $\left(V(\vec{r})\right)$;

$$\eta = \left(\frac{\partial \mu}{\partial N}\right)_{V(\vec{r})} = \left(\frac{\partial^2 E}{\partial N^2}\right)_{V(\vec{r})} \quad (2)$$

According to the Mulliken [41,42] and Pearson [43] theories, the absolute electronegativity (χ) and absolute hardness (η) are expressed as,

$$\chi = \frac{(IE+EA)}{2} \quad (3)$$

$$\eta \approx \frac{(IE-EA)}{2} \quad (4)$$

In Equations (3) and (4), IE and EA are, respectively. Chemical potential and electronegativity can be correlated [44] as,

$$\mu = -\chi$$

Hence,

$$\mu = -\chi \approx -\frac{(IE+EA)}{2} \quad (5)$$

By applying Koopmans [45] theorem and Kohn and Sham formalism [46] to DFT theory, the IE and EA can be expressed by E_{HOMO} and E_{LUMO}, respectively, having negative signs so, putting these terms in Equations (4) and (5), we get Equations (6) and (7);

$$\eta \approx \frac{(E_{LUMO} - E_{HOMO})}{2} \quad (6)$$

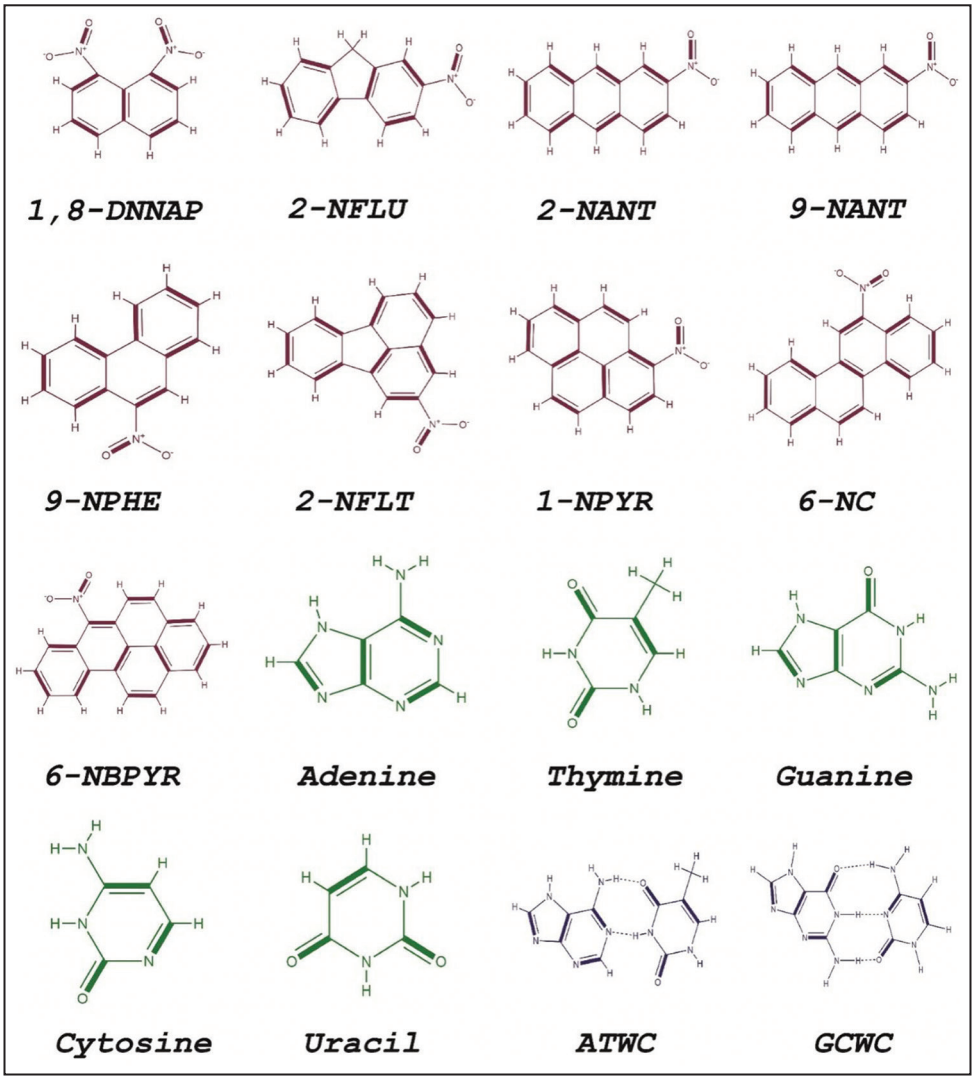

Figure 1: Molecular structures of nine nitro-polycyclic aromatic hydrocarbons and seven DNA/RNA bases and base pairs.

$$\mu \approx \frac{(E_{HOMO} + E_{LUMO})}{2} \quad (7)$$

When an electrophilic species or ligand is immersed in a sea of electron-rich media, ligand gets saturated and soaks up electrons until its chemical potential becomes same as that of electronic media, and consequently, ligand gets stabilized and reaches up to minimum energy. The ability of the ligand to accept electrons is defined by electrophilicity index (ω) and was introduced by Parr *et al*., in 1999 [35]. This term is expressed in Equation (8);

$$\omega = \frac{\mu^2}{2\eta} \quad (8)$$

In molecular systems, partial charge transfer occurs between electrophilic (acceptor) and nucleophilic (donor) molecules when they are brought together in a single system and the extent of electronic charge transfer can be determined by ΔN method [34] as expressed in Equation (9),

$$\Delta N_{MS} = \frac{(\mu_M - \mu_S)}{2(\eta_S + \eta_M)} \quad (9)$$

Where, M and S are the two different systems which interact with each other. If $\Delta N_{MS} < 0$, transfer of charge occurs from S to M (S-donor, M-acceptor), and if, $\Delta N_{MS} > 0$, charge flows from M to S (M-donor, S-acceptor).

Table 1: HOMO-LUMO energies (eV) and reactivity descriptors of NPAHs calculated at B3LYP/6-31G* level of theory.

NPAHs	Abbreviation	E_{HOMO}	E_{LUMO}	μ	η	ω	ΔN_{max}
1,8-dinitronaphthalene	1,8-DNNAP	−6.874	−2.575	−4.725	2.150	5.192	2.198
2-nitrofluorene	2-NFLU	−6.330	−2.274	−4.302	2.028	4.563	2.121
2-nitroanthracene	2-NANT	−5.724	−2.511	−4.118	1.607	5.277	2.563
9-nitroanthracene	9-NANT	−5.671	−2.328	−4.000	1.672	4.785	2.392
9-nitrophenanthrene	9-NPHE	−6.265	−2.337	−4.301	1.964	4.709	2.190
2-nitrofluoranthene	2-NFLT	−6.207	−2.494	−4.351	1.857	5.097	2.343
1-nitropyrene	1-NPYR	−5.805	−2.457	−4.131	1.674	5.097	2.468
6-nitrochrysene	6-NC	−5.952	−2.341	−4.147	1.806	4.761	2.296
6-nitrobenzo[a] pyrene	6-NBPYR	−5.502	−2.403	−3.953	1.550	5.041	2.550

NPAHs: Nitro-polycyclic aromatic hydrocarbons

Table 2: HOMO-LUMO energies (eV) and reactivity descriptors of DNA/RNA bases and base pairs calculated at B3LYP/6-31G* level of theory.

DNA/RNA bases and base pairs	E_{HOMO}	E_{LUMO}	μ	η	ω	ΔN_{max}
Adenine	−5.875	−0.412	−3.144	2.732	1.809	1.151
Thymine	−6.467	−0.916	−3.692	2.776	2.455	1.33
Guanine	−5.581	−0.088	−2.835	2.747	1.463	1.032
Cytosine	−6.092	−0.77	−3.431	2.661	2.212	1.289
Uracil	−6.768	−1.071	−3.92	2.849	2.697	1.376
ATWC	−5.698	−0.794	−3.246	2.452	2.149	1.324
GCWC	−4.956	−1.153	−3.055	1.902	2.453	1.606

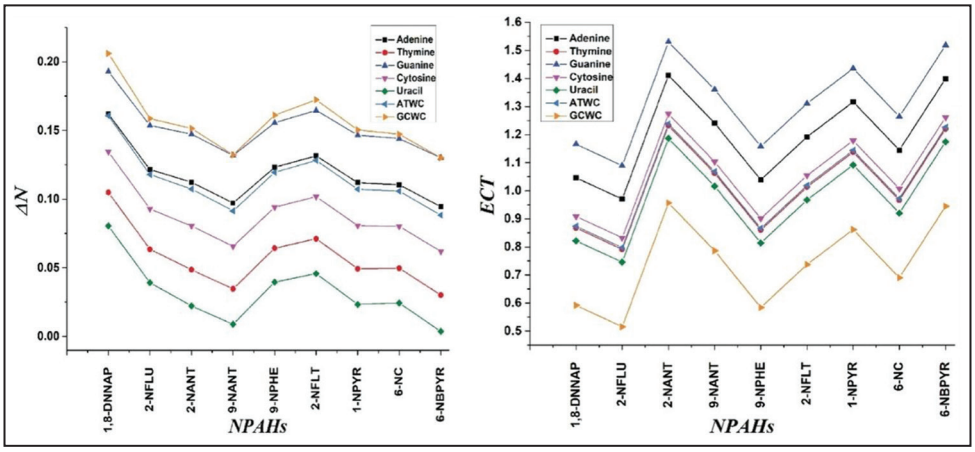

Figure 2: Charge transfer (eV) between nitro-polycyclic aromatic hydrocarbons and DNA/RNA bases and base pairs based on ΔN and ECT methods at B3LYP/6-31G* level of theory.

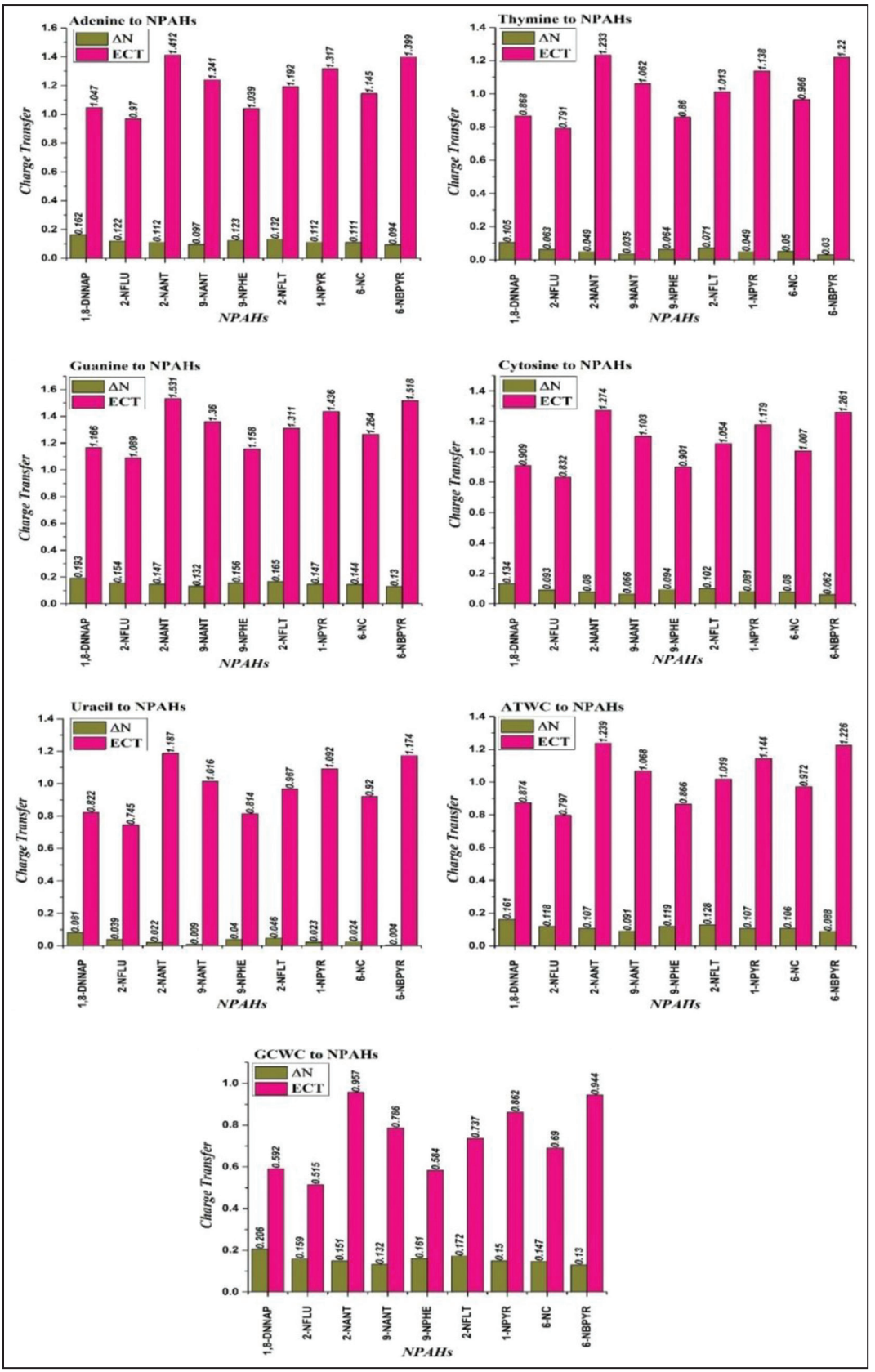

Figure 3: Comparison of charge transfer (eV) from each DNA/RNA base and base pair to nine nitro-polycyclic aromatic hydrocarbons by ΔN and ECT methods.

In 2007, Padmanabhan *et al*. proposed a new model called ECT [36] which defines the maximum charge accepting ability of species from its chemical environment. This can be mathematically expressed as;

$$ECT=(\Delta N_{max})_S-(\Delta N_{max})_M \quad (10)$$

In this model, if ECT < 0, charge transfers from S to M (S-donor, M-acceptor) and if ECT > 0, charge transfers from M to S (M-donor, S-acceptor).

Where, ΔN_{max} term was introduced by Parr *et al*. [35] which is the ratio of chemical potential and chemical hardness;

$$\Delta N_{max}=-\frac{\mu}{\eta} \quad (11)$$

2.2 Computational Details

The ORCA 4.0.1 Ab initio program [47] was used to calculate the electronic properties of the molecular system. The Avogadro 1.2.0 molecular editing software [48] was used to generate all input files. There was no symmetry restriction used while optimization of structures. The molecular geometry of NPAHs and DNA/RNA bases and base pairs was optimized using DFT hybrid functional, B3LYP [49,50] and Pople basis set 6-31G* [51]. The ground states of molecules were confirmed by the absence of negative frequency in the output files. In binding energy calculation, the geometrical counterpoise (gCP) correction [52] and dispersion correction [53,54] were carried out using gCP-D3 web service [55,56]. The binding energies of ATWC-NPAHs and GCWC-NPAHs complexes were computed using the supermolecule approach [57] and the AIM [58] analysis was performed using Multiwfn 3.3.6 program [59] at the same level of DFT theory. During the optimization of geometry, RIJCOSX approximation [60,61] was used and all the calculations were carried out in gas-phase geometry.

3. RESULTS AND DISCUSSION

The Kohn and Sham DFT (KS-DFT) is widely used by researchers and the B3LYP hybrid functional has become popular among the scientific community in the field of computational chemistry to investigate various structural [62,63], spectroscopic [64-70], and thermodynamic [71-74] properties of molecules and non-covalent interactions [75-79] between molecular systems. Furthermore, the B3LYP functional with Gaussian basis set 6-31G* has been used to calculate various molecular properties in literature [80-85].

3.1. Charge-transfer Interactions

The charge-transfer interactions between nine NPAHs and seven DNA/ RNA bases and base pairs have been investigated using ΔN [34] and ECT [36] methods. The HOMO-LUMO energies and magnitudes of reactive descriptors such as chemical potential (μ), chemical hardness (η), electrophilicity index (ω), and maximum charge transfer (N_{max}) for NPAHs and DNA/RNA bases and base pairs are shown in Tables 1 and 2, respectively, while Tables 3 and 4 indicate the calculated charge transfer between these two systems by ΔN and ECT methods, respectively.

Table 3: Charge transfer (eV) between NPAHs and DNA/RNA bases and base pairs by ΔN method calculated at B3LYP/6-31G* level of theory.

DNA/RNA bases and base pairs							
NPAHs	**Adenine**	**Thymine**	**Guanine**	**Cytosine**	**Uracil**	**ATWC**	**GCWC**
1,8-DNNAP	0.162	0.105	0.193	0.134	0.081	0.161	0.206
2-NFLU	0.122	0.063	0.154	0.093	0.039	0.118	0.159
2-NANT	0.112	0.049	0.147	0.080	0.022	0.107	0.151
9-NANT	0.097	0.035	0.132	0.066	0.009	0.091	0.132
9-NPHE	0.123	0.064	0.156	0.094	0.040	0.119	0.161
2-NFLT	0.132	0.071	0.165	0.102	0.046	0.128	0.172
1-NPYR	0.112	0.049	0.147	0.081	0.023	0.107	0.150
6-NC	0.111	0.050	0.144	0.080	0.024	0.106	0.147
6-NBPYR	0.094	0.030	0.130	0.062	0.004	0.088	0.130

NPAHs: Nitro-polycyclic aromatic hydrocarbons

Table 4: Charge transfer (eV) between NPAHs and DNA/RNA bases and base pairs by ECT method calculated at B3LYP/6-31G* level of theory.

DNA/RNA bases and base pairs							
NPAHs	**Adenine**	**Thymine**	**Guanine**	**Cytosine**	**Uracil**	**ATWC**	**GCWC**
1,8-DNNAP	1.047	0.868	1.166	0.909	0.822	0.874	0.592
2-NFLU	0.970	0.791	1.089	0.832	0.745	0.797	0.515
2-NANT	1.412	1.233	1.531	1.274	1.187	1.239	0.957
9-NANT	1.241	1.062	1.360	1.103	1.016	1.068	0.786
9-NPHE	1.039	0.860	1.158	0.901	0.814	0.866	0.584
2-NFLT	1.192	1.013	1.311	1.054	0.967	1.019	0.737
1-NPYR	1.317	1.138	1.436	1.179	1.092	1.144	0.862
6-NC	1.145	0.966	1.264	1.007	0.920	0.972	0.690
6-NBPYR	1.399	1.220	1.518	1.261	1.174	1.226	0.944

NPAHs: Nitro-polycyclic aromatic hydrocarbons

By comparing the values of reactivity descriptors in Tables 1 and 2, it can be concluded that the chemical potential (μ) and electrophilicity index (ω) values of NPAHs are greater in magnitude than DNA/RNA bases and base pairs. In a system, wherein NPAHs and DNA/RNA bases and base pairs are brought together, the former have a higher tendency for electrons and behave as an electron acceptor, whereas the latter act as an electron donor.

Hence, NPAHs will receive a fraction of charge from their neighboring DNA/RNA bases and base pairs. The charge transfer occurs until the system reaches equilibrium. After this, the system will have a single chemical potential [35].

Figure 2 illustrates the magnitude and pattern of charge transfer between NPAHs and DNA/RNA bases and base pairs, whereas Figure 3 compares the amount of charge transfer using both ΔN and ECT methods for each base and base pair with nine NPAHs. It can be clearly shown from Figure 2, the ECT method has significantly higher values of charge transfer than ΔN method. Furthermore, both methods predict different results for charge transfer. The maximum charge transfer in case of ΔN method was observed for GCWC base pair while in ECT method, it was observed for Guanine base, but the minimum charge transfer occurs for uracil in ΔN method and for GCWC base pair in

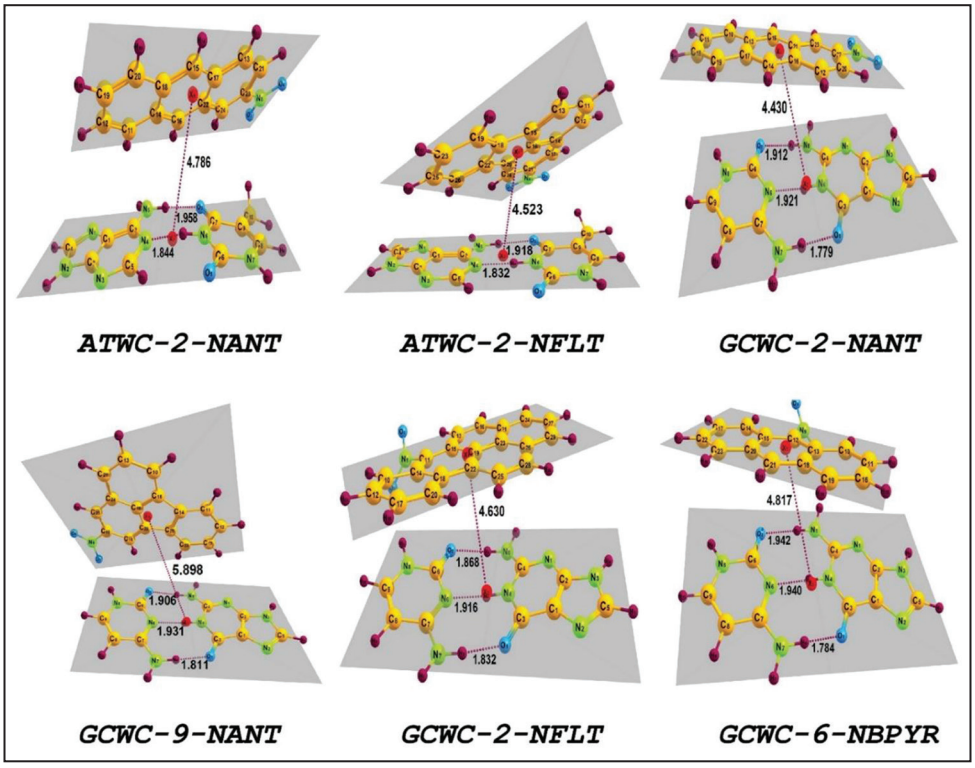

Figure 4: Optimized structures of ATWC-nitro-polycyclic aromatic hydrocarbons (NPAHs) and GCWC-NPAHs complexes at B3LYP/6-31G* level of theory.

Table 5: gCP and D3 corrected SCF energies (kcal/mol) of NPAHs, DNA/RNA bases and base pairs, and complexes (ATWC-NPAHs and GCWC-NPAHs) calculated at B3LYP/6-31G* level of theory.

Complexes	SCF energy	gCP correction	D3 correction	gCP-D3 correction	SCF-gCP-D3 energy
2-NANT	−466,608.914	32.841	−37.853	−5.012	−466,613.926
9-NANT	−466,601.104	33.455	−39.050	−5.595	−466,606.699
2-NFLT	−514,407.873	34.575	−43.108	−8.533	−514,416.406
6-NBPYR	−610,763.256	43.210	−57.625	−14.415	−610,777.671
ATWC	−577,909.405	47.304	−37.291	10.013	−577,899.392
GCWC	−587,977.536	48.150	−37.064	11.085	−587,966.450
ATWC-2-NANT	−1,044,520.861	82.887	−83.807	−0.921	−1,044,521.782
ATWC-2-NFLT	−1,092,319.678	85.986	−90.362	−4.376	−1,092,324.055
GCWC-2-NANT	−1,054,588.455	85.185	−88.226	−3.041	−1,054,591.496
GCWC-9-NANT	−1,054,580.989	84.717	−85.348	−0.631	−1,054,581.620
GCWC-2-NFLT	−1,102,393.453	86.516	−87.660	−1.144	−1,102,394.597
GCWC-6-NBPYR	−1,198,745.837	95.412	−108.318	−12.907	−1,198,758.743

NPAHs: Nitro-polycyclic aromatic hydrocarbons, SCF: Self-consisted field

ECT method. The charge transfer values calculated by both the methods are positive in magnitude which indicates that the fraction of charge flows from system M (DNA/RNA bases and base pairs) to system S (NPAHs).

For ΔN method, 1,8-dinitronaphthalene accepts the higher charge from all bases and base pairs compared to the other NPAHs. In contrast to that, 6-Nitrobenzo[a]pyrene gets a significantly lower amount of charge from bases and base pairs.

9-nitroanthracene gets only a slightly higher proportion of charge than 6-Nitrobenzo[a]pyrene. 2-nitrofluoranthene also receives a greater amount of charge but considerably lower than 1,8-dinitronaphthalene. The proportion of charge transfer from bases and base pairs to 2-nitroanthracene, 1-nitropyrene, and 6-nitrochrysene is equal in magnitudes.

In ECT method, 2-nitroanthracene and 6-nitrobenzo[a]pyrene have strong charge-transfer interactions with bases and base pairs, and consequently, charge flows from bases and base pairs to these two NPAHs are remarkably greater than other NPAHs. 1-nitropyrene is the third most interacting species with bases and base pairs. 2-nitrofluorene has the least interactions with bases and base pairs so charge transfer between the two is substantially less in magnitudes. The charge transfer to 1,8-dinitronaphthalene and 9-nitrophenanthrene is almost equal in magnitude. The remaining three NPAHs, namely, 9-nitroanthracene, 2-nitrofluoranthene, and 6-nitrochrysene interact moderately with bases and base pairs.

Table 6: Intermolecular distances (*R* in Å), gCP and D3 uncorrected and corrected binding energies (kcal/mol) of ATWC-NPAHs and GCWC-NPAHs complexes calculated at B3LYP/6-31G* level of theory.

Complexes	R(Å)	Uncorrected E_b	Corrected E_b
ATWC-2-NANT	4.786	−2.542	−8.464
ATWC-2-NFLT	4.523	−2.400	−8.257
GCWC-2-NANT	4.430	−2.006	−11.120
GCWC-9-NANT	4.817	−2.350	−8.471
GCWC-2-NFLT	5.898	−8.044	−11.741
GCWC-6-NBPYR	4.630	−5.045	−14.622

NPAHs: Nitro-polycyclic aromatic hydrocarbons

3.2 Binding Energy

The optimized complexes, ATWC-NPAHs and GCWC-NPAHs, are shown in Figure 4. To measure the intermolecular distances in the complexes, the red dummy atom was put in the center of each monomer. Table 5 represents the gCP-D3 corrected and uncorrected self-consisted field energies of NPAHs, DNA/RNA bases and base pairs, and the complexes of ATWC-NPAHs and GCWC-NPAHs, whereas corrected and uncorrected binding energies of these complexes are summarized in Table 6.

The binding energies of ATWC-NPAHs and GCWC-NPAHs complexes were calculated by supermolecule approach [57], in which initially, the geometry of NPAHs and base pairs (ATWC and GCWC) was optimized individually at the B3LYP/6-31G* level of DFT theory, and finally, their complexes were optimized at the same level of theory without any geometry constraint. Binding energies (E_b) of complexes were calculated from Equation (12),

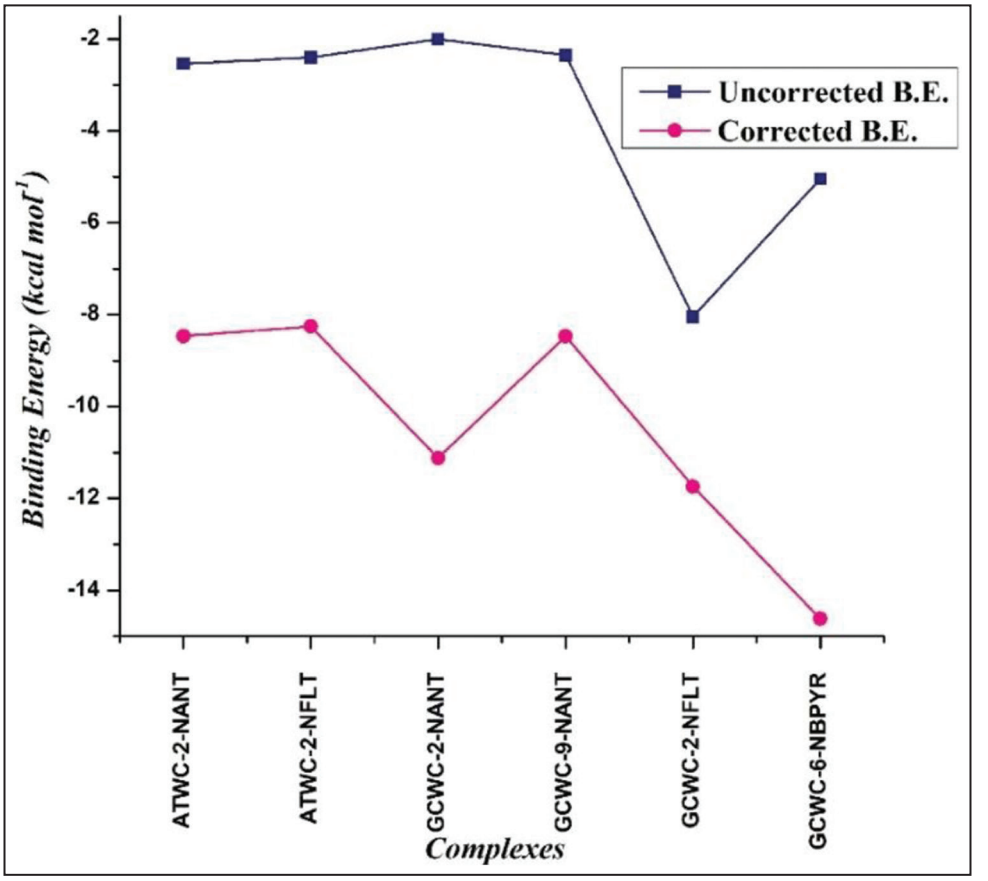

Figure 5: Uncorrected and corrected binding energies (kcal/mol) of ATWC-nitro-polycyclic aromatic hydrocarbons (NPAHs) and GCWC-NPAHs complexes at B3LYP/6-31G* level of theory.

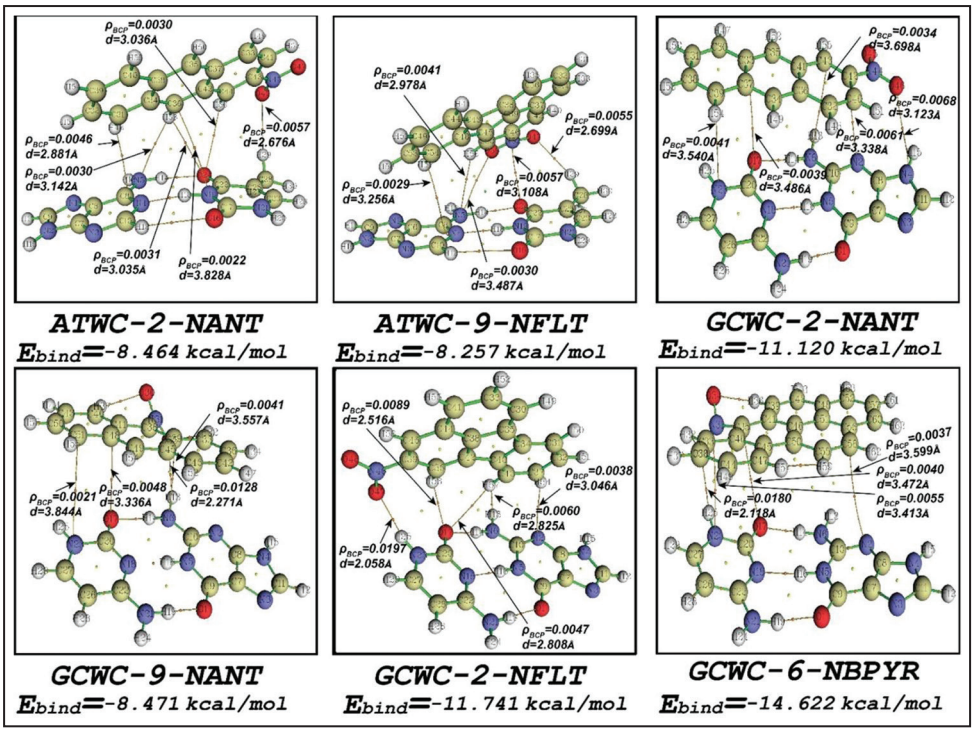

Figure 6: Molecular graphs (AIM) of ATWC-nitro-polycyclic aromatic hydrocarbons (NPAHs) and GCWC-NPAHs complexes calculated at B3LYP/6-31G* level of theory.

$$E_b = E^{OPT}_{COMPLEX} - \left(E^{OPT}_{BASE\ PAIR} + E^{OPT}_{NPAH}\right) \quad (12)$$

Where, $E^{OPT}_{COMPLEX}$ is the optimized energy of complex and $E^{OPT}_{BASE\ PAIR}$ and E^{OPT}_{NPAH} are optimized energies of base pair and NPAH, respectively.

In B3LYP/6-31G* hybrid functional, the long-range London dispersion interactions are ignored. Hence, Stefan Grimme *et al*. [53,54] constructed a new method DFT-D/DFT-D3 to correct the calculations by including dispersion electron correlations.

It is also observed geometrical inter- and intra-molecular basis set superposition error (BSSE) in density functional and Hartree–Fock methods and to overcome this error, Kruse and Grimme [52] developed gCP correction method. Kruse *et al*. have developed web service [55,56] for combined correction of BSSE and dispersion corrections without any extended computational time.

Figure 5 demonstrates a significant difference in uncorrected and corrected binding energies of the ATWC-NPAHs and GCWC-NPAHs complexes. The gCP-D3 corrected values of binding energies are more negative than uncorrected values which indicate greater stability of the complexes. The magnitude of binding energies ranges from 2 to 9 kcal/ mol and 8 to 15 kcal/mol, respectively, for uncorrected and corrected binding energies. In the case of uncorrected binding energies, the most stable complex is GCWC-2-NFLT (E_b=−8.044 kcal/mol) while the least stable complex is GCWC-2-NANT (E_b=−2.006 kcal/mol). However, for gCP-D3 corrected binding energies, the 6-NBPYR binds strongly (E_b=−14.622 kcal/mol) to GCWC base pair, while 2-NFLT has weak binding (E_b=−8.257 kcal/mol) with ATWC base pair. Three complexes, ATWC-2-NANT, ATWC-2-NFLT, and GCWC-9-NANT, have a relatively small and similar magnitude of binding energies around −8.500 kcal/mol, whereas, GCWC-2-NANT and GCWC-2-NFLT complexes have a significantly higher magnitude of binding energies but less than the GCWC-6-NBPYR complex.

3.3. AIM Analysis

The AIM molecular graphs of complexes with bond critical points (BCPs) in orange and ring critical points (RCPs) in yellow color are represented in Figure 6. The topological analysis of electron density of ATWC-NPAHs and GCWC-NPAHs complexes was examined at B3LYP/6-31G* level. Table 7 represents the calculated topological electron density parameters such as interatomic distances (d in Å), kinetic energy ($G(r_c)$), potential energy density ($V(r_c)$), all electron density (ρ_{BCP}), Laplacian of electron density ($\nabla^2\rho_{BCP}$), and the ratio of kinetic energy and potential energy density ($G(r_c)/(V(r_c))$. From the results, six different types of bonding are identified which includes hydrogen bonding (N---H and O---H) and other bonding such as N---C, O---C, O---N, and C---H. The calculated H-bonding distances are found between 2.058 Å and 3.256 Å, whereas other bond distances are between 2.881 Å and 3.828 Å.

To confirm the types of interactions, various concepts have been reported. If the electron density (ρ_{BCP}) values are greater than the order of 10^{-1}a.u. at BCP and the values of Laplacian of electron density ($\nabla^2\rho_{BCP}$) are negative, interactions are purely in covalent nature. Furthermore, if the value of $|V(r_c)|$ is less than the twice the value of $G(r_c)$ [$|V(r_c)| < 2G(r_c)$] and the ratio of $G(r_c)$ and $V(r_c)$ [$-G(r_c)/V(r_c)$] is greater than the unity; then, the interactions are non-covalent in nature [86]. The magnitude of electron density (ρ_{BCP}) at BCP is low, ranging from 0.0021 to 0.0197 a.u., indicating that the non-covalent interactions should be established between the monomers in the ATWC-NPAHs and GCWC-NPAHs complexes. In Table 7, the $\nabla^2\rho_{BCP}$ values are positive and lower in magnitude, so the interactions are non-covalent in nature.

Furthermore, the values of $|V(r_c)|$ are less than twice the values of $G(r_c)$ and the ratio is found greater than unity which indicate the non-covalent interactions between monomers.

Table 7: Interatomic distances (d in Å), kinetic energy (G (r_c)), potential energy density (V (r_c)), electrons density (ρ_{BCP}), Laplacian of electron density ($\nabla^2\rho_{BCP}$), and ratio (−G (r_c)/V (r_c)) of ATWC-NPAHs and GCWC-NPAHs complexes are in a.u. calculated at B3LYP/6-31G* level of theory.

Complexes	Bond	Distance (*d*)	*G* (r_c)	*V* (r_c)	ρ_{BCP}	$\nabla^2\rho_{BCP}$	-*G* (r_c)/*V* (r_c)
ATWC-2-NANT	N19-C36	3.8280	0.0015	−0.0012	0.0022	0.0077	1.2500
	C8-H48	2.8810	0.0033	−0.0023	0.0046	0.0177	1.4348
	O24-H53	3.0350	0.0024	−0.0016	0.0031	0.0128	1.5000
	O24-H56	3.0360	0.0023	−0.0015	0.0030	0.0124	1.5333
	N5-H53	3.1420	0.0020	−0.0014	0.0030	0.0102	1.4286
	O46-H29	2.6760	0.0043	−0.0034	0.0057	0.0206	1.2647
ATWC-2-NFLT	N4-H57	3.2560	0.0020	−0.0014	0.0029	0.0102	1.4286
	O47-H29	2.6990	0.0042	−0.0033	0.0055	0.0203	1.2727
	O24-N52	3.1080	0.0048	−0.0039	0.0057	0.0229	1.2308
	N5-H56	2.9780	0.0028	−0.0021	0.0041	0.0138	1.3333
	N5-O55	3.4870	0.0026	−0.0020	0.0030	0.0129	1.3000
GCWC-2-NANT	N23-C39	3.5400	0.0026	−0.0021	0.0041	0.0121	1.2381
	O17-C37	3.4860	0.0028	−0.0021	0.0039	0.0141	1.3333
	N6-C43	3.6980	0.0022	−0.0018	0.0034	0.0107	1.2222
	N2-C42	3.3380	0.0039	−0.0032	0.0061	0.0183	1.2188
	O46-N4	3.1230	0.0056	−0.0047	0.0068	0.0260	1.1915
GCWC-9-NANT	N23-C51	3.8440	0.0015	−0.0011	0.0021	0.0074	1.3636
	O17-C48	3.3360	0.0036	−0.0028	0.0048	0.0172	1.2857
	N6-C39	3.5570	0.0027	−0.0022	0.0041	0.0128	1.2273
	O35-H13	2.2710	0.0106	−0.0100	0.0128	0.0446	1.0600
GCWC-2-NFLT	O47-H25	2.0580	0.0161	−0.0162	0.0197	0.0645	0.9938
	O17-H53	2.5160	0.0068	−0.0060	0.0089	0.0304	1.1333
	O17-H57	2.8080	0.0036	−0.0026	0.0047	0.0181	1.3846
	N6-H57	2.8250	0.0040	−0.0032	0.0060	0.0188	1.2500
	N2-H54	3.0460	0.0024	−0.0018	0.0038	0.0121	1.3333
GCWC-6-NBPYR	O30-H25	2.1180	0.0145	−0.0146	0.0180	0.0575	0.9932
	N23-C33	3.4130	0.0035	−0.0030	0.0055	0.0163	1.1667
	O17-C35	3.4720	0.0029	−0.0023	0.0040	0.0144	1.2609
	N2-C58	3.5990	0.0023	−0.0018	0.0037	0.0110	1.2778

NPAHs: Nitro-polycyclic aromatic hydrocarbons

4. CONCLUSION

The charge transfer between nine NPAHs and seven DNA/RNA bases and base pairs was investigated using Δ*N* and *ECT* methods. In the system, since electrophilicity index (ω) values of NPAHs are higher in magnitude compared to those of DNA/RNA bases and base pairs, charge flows from bases and base pairs to NPAHs. ΔN and *ECT* methods give different results for charge transfer. NPAHs have a different binding affinity with ATWC and GCWC base pairs. The AIM topological analysis confirms the presence of non-covalent interactions in these complexes as evident from the values of BCP and RCP. Donor and acceptor components form H-bonding (due to N and O atoms) and other types of bonding such as N---C, O---C, O---N, and C---H in the complexes.

5. REFERENCES

1. W. Wang, N. Jariyasopit, J. Schrlau, Y. Jia, S. Tao, T. Yu, R. H. Dashwood, W. Zhang, X. Wang, S. L. M. Simonich, (2011) Concentration and photochemistry of PAHs, NPAHs, and OPAHs and toxicity of $PM_{2.5}$ during the Beijing Olympic games, ***Environmental Science and Technology*, 45:** 6887-6895.
2. W. Huang, B. Huang, X. Bi, Q. Lin, M. Liu, Z. Ren, G. Zhang, X. Wang, G. Sheng, J. Fu, (2014) Emission of PAHs, NPAHs and OPAHs from residential honeycomb coal briquette combustion, ***Energy Fuels*, 28:** 636-642.
3. C. Hung, H. Ho, M. Lin, C. Chen, Y. Shu, M. Lee, (2012) Purge-assisted headspace solid-phase microextraction combined with gas chromatography/mass spectrometry for the determination of trace nitrated polycyclic aromatic hydrocarbons in aqueous samples, ***Journal of Chromatography A*, 1265:** 1-6.
4. J. L. Durant, W.F. Busby Jr., A. L. Lafleur, B. W. Penman, C. L. Crespi, (1996) Human cell mutagenicity of oxygenated, nitrated and unsubstituted polycyclic aromatic hydrocarbons associated with urban aerosols, ***Mutation Research*, 371:** 123-157.
5. J. Zhang, L. Yang, A. Mellouki, J. Chen, X. Chen, Y. Gao, P. Jiang, Y. Li, H. Yu, W. Wang, (2018) Diurnal concentrations, sources, and

cancer risk assessments of $PM_{2.5}$ bound PAHs, NPAHs, and OPAHs in urban, marine and mountain environments, ***Chemosphere*, 209:** 147-155.

6. X. Hao, X. Zhang, X. Cao, X. Shen, J. Shi, Z. Yao, (2018) Characterization and carcinogenic risk assessment of polycyclic aromatic and nitro polycyclic aromatic hydrocarbons in exhaust emission from gasoline passenger cars using on-road measurements in Beijing, China, ***Science of Total Environment*, 645:** 347-355.
7. B. Huang, M. Liu, X. Bi, C. Chaemfa, Z. Ren, X. Wang, G. Sheng, J. Fu, (2014) Phase distribution, sources and risk assessment of PAHs, NPAHs and OPAHs in a rural site of Pearl River Delta region, China, ***Atmospheric Pollution Research*, 5:** 210-218.
8. W. J. Dunn 3rd, (1988) QSAR approaches to predicting toxicity, ***Toxicology Letters*, 43:** 277-283.
9. L. Jiang, L. Lai, (2002) CH···O Hydrogen bonds at protein-protein interfaces, ***The Journal of Biological Chemistry*, 277:** 37732-37740.
10. D. Xu, C. Tsai, R. Nussinov, (1997) Hydrogen bonds and salt bridge across protein-protein interfaces, ***Protein Engineering*, 9:** 999-1012.
11. R. P. Bywater, (2017) A tensegrity model for hydrogen bond networks in proteins, ***Heliyon*, 4**: e00307.
12. A. Bondar, S. H. White, (2012) Hydrogen bond dynamics in membrane protein function, ***Biochimica etBiophysica Acta*, 1818:** 942-950.
13. R. S. Mulliken, (1950) Structures of complexes formed by halogen molecules with aromatic and with oxygenated solvents, ***Journal of the American Chemical Society,* 72:** 600-608.
14. P. Politzer, P. Lane, M. C. Concha, Y. Ma, J. S. Murray, (2007) An overview of halogen bonding, ***Journal of Molecular Modeling,* 13:** 305-311.
15. P. Metrangolo, F. Meyer, T. Pilati, G. Resnati, G. Terraneo, (2008) Halogen bonding in supramolecular chemistry, ***Angewandte Chemie International Edition*, 47:** 6114-6127.
16. R. M. Minyaev, V. I. Minkin, (1998) Theoretical study of O - > X (S, Se, Te) coordination in organic compounds, ***Canadian Journal Chemistry*, 76:** 776-788.
17. O. Mó, P. Sanz, M. Yáñez, (2002) 1,8-Chalcogen-bridged naphthalenes. Strong carbon bases in the gas phase, ***New Journal of Chemistry*, 26:** 1747-1752.
18. O. Mó, P. Sanz, M. Yáñez, (2003) Characterization of intramolecular hydrogen bonds and competitive chalcogen-chalcogen interactions on the basis of the topology of the charge density, ***Physical Chemistry Chemical Physics,* 5:** 2942-2947.
19. K. W. Klinkhammer, P. Pyykkö, (1995) Ab initio interpretation of the closed-shell intermolecular E···E attraction in dipnicogen $(H_2E\text{-}EH_2)_2$ and dichalcogen $(HE\text{-}EH)_2$ hydride model dimers, ***Inorganic Chemistry*, 34:** 4134-4138.
20. F. B. Alhanash, N. A. Barnes, A. K. Brisdon, S. M. Godfrey, R. G. Pritchard, (2012) Formation of M_4Se_4 cuboids (M = As, Sb, Bi) via secondary pnictogen-chalcogen interactions in the co-crystals $MX_3{\cdot}Se{=}P(p\text{-}FC_6H_4)_3$ (M = As, X = Br; M = Sb, X = Cl; M = Bi, X = Cl, Br), ***Dalton Transactions*, 41:** 10211-10218.
21. J. Moilanen, C. Ganesamoorthy, M. S. Balakrishna, H. M. Tuononen, (2009) Weak interactions between trivalent pnictogen centers: Computational analysis of bonding in dimers $X_3E{\cdots}EX_3$ (E = Pnictogen, X = Halogen), ***Inorganic Chemistry*, 48:** 6740-6747.
22. S. Zahn, R. Frank, E. Hey-hawkins, B. Kirchner, (2011) Pnicogen bonds: A new molecular linker? ***Chemistry A European Journal*, 17:** 6034-6038.
23. J. Poater, M. Swart, F. M. Bickelhaupt, C. F. Guerra, (2014) B-DNA structure and stability: The role of hydrogen bonding, π-π stacking interactions, twist-angle, and solvation, ***Organic Biomolecular Chemistry*, 12:** 4691-4700.
24. M. O. Sinnokrot, E. F. Valeev, C. D. Sherrill, (2002) Estimates of the Ab initio limit for π - π interactions: The benzene dimer, ***Journal American Chemical Society*, 124:** 10887-10893.
25. M. O. Sinnokrot, C. D. Sherrill, (2003) Unexpected substituent effects in face-to-face π-stacking interactions, ***The Journal of Physical Chemistry A*, 107:** 8377-8379.
26. N. Sathyamurthy, B. K. Mishra, (2006) Stacking interaction in pyrazine dimer, ***Journal of Theoretical Computer Chemistry*, 5:** 609-619.
27. A. Farrokhzadeh, A. R. Modarresi-alam, F. B. Akher, A. Ebrahimi, (2016) A theoretical study of π-stacking interactions in C-substituted tetrazoles, ***Journal of Molecular Graphics Modelling*, 67:** 85-93.
28. N. O. Dubinets, A. A. Safonov, A. A. Bagaturyants, (2016) Structures and binding energies of the naphthalene dimer in its ground and excited states, ***The Journal of Physical Chemistry A*, 120:** 2779-2782.
29. F. B. Akher, A. Ebrahimi, N. Mostafavi, (2017) Characterization of π-stacking interactions between aromatic amino acids and quercetagetin, ***Journal of Molecular Structure*, 1128:** 13-20.
30. P. Hobza, J. Šponer, (2002) Toward true DNA base-stacking energies: MP2, CCSD (T), and complete basis set calculations, ***Journal of American Chemical Society*, 124:** 11802-11808.
31. C. Trujillo, G. Sánchez-Sanz, (2016) A study of π-π stacking interactions and aromaticity in polycyclic aromatic hydrocarbon/nucleobase complexes, ***Chemphyschem*, 17:** 395-405.
32. P. P. Fu, D. Herreno-saenz, L. S. V. Tungeln, J. O. Lay, Y. Wu, J. S. Lai, F. E. Evans, (1994) DNA adducts and carcinogenicity of nitro-polycyclic aromatic hydrocarbons, ***Environmental Health Perspectives*, 102:** 177-183.
33. J. Padmanabhan, R. Parthasarathi, M. Elango, V. Subramanian, B. S. Krishnamoorthy, S. Gutierrez-Oliva, A. Toro-Labbé, D. R. Roy, P. K. Chattaraj, (2007) Multiphilic descriptor for chemical reactivity and selectivity, ***The Journal of Physical Chemistry A*, 111:** 9130-9138.
34. R. G. Parr, R. G. Pearson, (1983) Absolute hardness: Companion parameter to absolute electronegativity, ***Journal of American Chemical Society*, 105:** 7512-7516.
35. R. G. Parr, L. V. Szentpály, S. Liu, (1999) Electrophilicity index, ***Journal of American Chemical Society*, 121:** 1922-1924.
36. J. Padmanabhan, R. Parthasarathi, V. Subramanian, P. K. Chattaraj, (2007) Electrophilicity-based charge transfer descriptor, ***The Journal of Physical Chemistry A*, 111:** 1358-1361.
37. D. R. Roy, U. Sarkar, P. K. Chattaraj, A. Mitra, J. Padmanabhan, R. Parthasarathi, V. Subramanian, S. V. Damme, P. Bultinck, (2006) Analyzing toxicity through electrophilicity, ***Molecular Diversity*, 10:** 119-131.
38. U. Sarkar, D. R. Roy, P. K. Chattaraj, R. Parthasarathi, J. Padmanabhan, V. Subramanian, (2005) A conceptual DFT approach towards analysing toxicity, ***Journal Chemical Sciences*, 117:** 599-612.
39. F. B. Rizwana, J. C. Prasana, S. Muthu, C. S. Abraham, (2019) Molecular docking studies, charge transfer excitation and wave function analyses (ESP, ELF, LOL) on valacyclovir: A potential antiviral drug, ***Computational Biology and Chemistry*, 78:** 9-17.

40. S. Ash, H. Beg, P. Mazumdar, G. Salgado-Morán, A. Misra, (2014) Polarizability, hardness and electrophilicity as global descriptors for intramolecular proton transfer reaction path, ***Computational and Theoretical Chemistry*****, 1031:** 50-55.
41. R. S. Mulliken, (1934) A New Electroaffinity scale; together with data on valence states and on valence ionization potentials and electron affinities, ***The Journal of Chemical Physics*****, 2:** 782-793.
42. R. S. Mulliken, (1935) Electronic structures of molecules XI. electroaffinity, molecular orbitals and dipole moments, ***The Journal of Chemical Physics*****, 3:** 573-585.
43. R. G. Pearson, (1985) Absolute electronegativity and absolute hardness of Lewis acids and bases, ***Journal of the American Chemical Society*****, 107:** 6801-6806.
44. L. R. Domingo, M. Ríos-gutiérrez, P. Pérez, (2016) Applications of the conceptual density functional theory indices to organic chemistry reactivity**,** ***Molecules*****, 21:** 748.
45. T. Koopmans, (1934) Über die zuordnung von wellenfunktionen und eigenwertenzu den einzelnen elektronen eines atoms. ***Physica*****, 1:** 104-113.
46. W. Kohn, L. J. Sham, (1965) Self-consistent equations including exchange and correlation effects, ***Physical Review*****, 140**: A1133-A1138.
47. F. Neese, (2018) Software update: The ORCA program system, version 4.0, ***Wiley Interdisciplinary Reviews: Computational Molecular Science*****, 8**: e1327.
48. M. D. Hanwell, D. E. Curtis, D. C. Lonie, T. Vandermeersch, E. Zurek, G. R. Hutchison, (2012) Avogadro: An advanced semantic chemical editor, visualization, and analysis platform, ***Journal of Cheminformatics,*** **4:** 17.
49. C. Lee, W. Yang, R. G. Parr, (1988) Development of the Collesalvetti correlation-energy formula into a functional of the electron density, ***Physical Review B*****, 37:** 785-789.
50. A. D. Becke, (1993) Density-functional thermochemistry. III. The role of exact exchange, ***The Journal of Chemical Physics*****, 98:** 5648-5652.
51. R. Ditchfield, W. J. Hehre, J. A. Pople, (1971) Self-consistent molecular-orbital methods. IX. An extended Gaussian-type basis for molecular-orbital studies of organic molecules, ***The Journal of Chemical Physics*****, 54:** 724-728.
52. H. Kruse, S. Grimme, (2012) A geometrical correction for the inter- and intra-molecular basis set superposition error in Hartree-Fock and density functional theory calculations for large systems, ***The Journal of Chemical Physics*****, 136:** 154101.
53. S. Grimme, (2006) Semiempirical GGA-type density functional constructed with a long-range dispersion correction, ***Journal of Computational Chemistry*****, 27:** 1787-1799.
54. S. Grimme, J. Antony, S. Ehrlich, H. Krieg, (2010) A consistent and accurate ab initio parametrization of density functional dispersion correction (DFT-D for the 94 elements H-Pu, ***The Journal of Chemical Physics*****, 132:** 154104.
55. gCP-D3 Webservice: A Geometrical Counterpoise Correction for Basis set Superposition Error (BSSE) and Dispersion Correction for London Density Functionals. Hartree-Fock and Semi-empirical Quantum Chemical Methods, 2019. Available from: http://wwwtc.thch.uni-bonn.de. [Last accessed on 2019 Feb 12].
56. H. Kruse, L. Goerigk, S. Grimme, (2012) Why the standard B3LYP/6-31G* model chemistry should not be used in DFT calculations of molecular thermochemistry: Understanding and correcting the problem, ***The Journal of Organic Chemistry,*** **77:** 10824-10834.
57. T. Janowski, A. R. Ford, P. Pulay, (2010) Accurate correlated calculation of the intermolecular potential surface in the coronene dimer, ***Molecular Physics*****, 108:** 249-257.
58. R. F. W. Bader, (1990) ***Atoms in Molecules: A Quantum Theory***, Oxford: Clarendon Press.
59. T. Lu, F. Chen, (2012) Multiwfn: A multifunctional wavefunction analyzer, ***Journal of Computational Chemistry*****, 33:** 580-592.
60. F. Neese, (2003) An improvement of the resolution of the identity approximation for the formation of the coulomb matrix, ***Journal of Computational Chemistry*****, 24:** 1740-1747.
61. F. Neese, F. Wennmohs, A. Hansen, U. Becker, (2009) Efficient, approximate and parallel Hartree-Fock and hybrid DFT calculations. A "chain-of-spheres" algorithm for the Hartree-Fock exchange, ***Chemical Physics*****, 356:** 98-109.
62. M. Remko, J. Bojarska, P. Ježko, W. Maniukiewicz, A. Olczak, (2013) Molecular structure of antihypertensive drug perindopril, its active metabolite perindoprilat and impurity F, ***Journal of Molecular Structure*****, 1036:** 292-297.
63. J. Kuta, S. Patchkovskii, M. Z. Zgierski, P. M. Kozlowski, (2006) Performance of DFT in modeling electronic and structural properties of cobalamins, ***Journal of Computational Chemistry*****, 27:** 1429-1437.
64. U. Salzner, (2013) Quantitatively correct UV-vis spectrum of ferrocene with TDB3LYP, ***Journal of Chemical Theory and Computation*****, 9:** 4064-4073.
65. M. Govindarajan, K. Ganasan, S. Periandy, S. Mohan, (2010) DFT (LSDA, B3LYP and B3PW91) comparative vibrational spectroscopic analysis of α-acetonaphthone, ***Spectrochimica Acta A: Molecular and Biomolecular Spectroscopy*****, 76:** 12-21.
66. M. Evecen, H. Tanak, F. Tinmaz, N. Dege, İ. Ö. İlhan, (2016) Experimental (XRD, IR and NMR) and theoretical investigations on 1-(2-nitrobenzoyl)3,5-bis(4-methoxyphenyl)-4,5-dihydro-1*H*-pyrazole, ***Journal of Molecular Structure*****, 1126:** 117-126.
67. E. Virtanen, A. Valkonen, J. Tamminen, E. Kolehmainen, (2003) Comparison of calculated DFT/B3LYP and experimental ^{13}C and ^{17}O NMR chemical shifts, Ab initio HF/6-31G* optimised structures, and single crystal X-ray structures of some substituted methyl 5β-cholan-24-oates, ***Journal of Molecular Structure*****, 650:** 201-212.
68. A. C. Costa Jr., G. F. Ondar, O. Versiane, J. M. Ramos, T. G. Santos, A. A. Martin, L. Raniero, G. G. A. Bussi, C. A. T. Soto, (2013) DFT: B3LYP/6-311G (d, p) vibrational analysis of bis -(diethyldithiocarbamate) zinc (II) and natural bond orbitals, ***Spectrochimica Acta A: Molecular and Biomolecular Spectroscopy*****, 105:** 251-258.
69. O. V. Cabral, C. A. Téllez, S. T. Giannerini, J. Felcman, (2005) Fourier-transform infrared spectrum of aspartate hydroxo-aqua nickel (II) complex and DFT-B3LYP/3-21G and 6-311G structural and vibrational calculations, ***Spectrochimica Acta A: Molecular and Biomolecular Spectroscopy*****, 61:** 337-345.
70. B. Komjáti, Á. Urai, S. Hosztafi, J. Kökösi, B. Kováts, J. Nagy, P. Horváth, (2016) Systematic study on the TD-DFT calculated electronic circular dichroism spectra of chiral aromatic nitro compounds: A comparison of B3LYP and CAM-B3LYP, ***Spectrochimica Acta A: Molecular and Biomolecular Spectroscopy*****, 155:** 95-102.
71. T. Giroday, M. M. Montero-campillo, N. Mora-Diez, (2014) Thermodynamic stability of PFOS: M06-2X and B3LYP comparison, ***Computational and Theoretical Chemistry*****, 1046:** 81-92.
72. L. A. Curtiss, K. Raghavachari, P. C. Redfern, J. A. Pople, (1997) Assessment of Gaussian-2 and density functional theories for the

computation of enthalpies of formation, ***The Journal of Chemical Physics*****, 106:** 1063-1079.

73. L. O. M. Ana Filipa, Santos, A. L. R. Silva, O. D. F. Santiago, J. M. Gonçalves, S. Pandey, W. E. Acree Jr., D. M. C. Maria, R. D. Silva, (2014) Thermochemical properties of 4-N, N-dialkylamino-7-nitrobenzofurazan derivatives (alkyl = methyl, ethyl), ***The Journal of Chemical Thermodynamics*****, 73:** 62-68.
74. G. Zhao, Y. Liu, W. Shi, T. Chai, F. Ren, (2014) A B3LYP and MP2 (full) theoretical investigation into cooperativity effects, aromaticity and thermodynamic properties in the Na^+... benzonitrile...H_2O ternary complex, ***Journal of Molecular Modeling*****, 20:** 1-13.
75. Z. Moosavi-Tekyeh, S. F. Tayyari, (2015) Theoretical and spectroscopic studies on molecular structure and hydrogen bonding of 2-trifluoroacetylphenol, ***Spectrochimica Acta A: Molecular and Biomolecular Spectroscopy*****, 135:** 820-827.
76. M. Lozynski, D. Rusinska-Roszak, H. Mack, (1998) Hydrogen bonding and density functional calculations: The B3LYP approach as the shortest way to MP2 results, **Journal *of Physical Chemistry A*****, 102:** 2899-2903.
77. Y. Wu, F. Ren, B. Li, (2009) A B3LYP and MP2 theoretical investigation on unusual cation-π interaction between the singlet state HB=BH ($^1\Delta_g$) and H^+, Li^+, Na^+, Be^{2+} or Mg^{2+}, ***Journal of Molecular Structure: THEOCHEM*****, 909:** 79-85.
78. B. K. Mishra, N. Sathyamurthy, (2005) π-π Interaction in pyridine, ***Journal of Physical Chemistry A*****, 109:** 6-8.
79. D. Cao, F. Ren, Y. Feng, S. Liu, S. Chen, (2010) A B3LYP and MP2 theoretical investigation into host-guest interaction between calix[4]arene and Li^+ or Na^+, ***Journal of Molecular Modeling*****, 16:** 589-598.
80. M. Kwiatkowska, R. Jasiński, A. Barański, (2009) A competition between carbo and hetero Diels-Alder reactions of E-2-phenyl-1-cyano-1-nitroethene to cyclopentadiene in the light of B3LYP/6-31G (d) computational study, ***Journal of Molecular Structure: THEOCHEM*****, 910:** 80-87.
81. G. Alagona, C. Ghio, S. Monti, (1998) The effect of small substituents on the properties of indole. An ab initio 6-31G* study, ***Journal of Molecular Structure: THEOCHEM*****, 433:** 203-216.
82. S. M. Bouzzine, S. Bouzakraoui, M. Bouachrine, M. Hamidi, (2005) Density functional theory (B3LYP/6-31G*) study of oligothiophenes in their aromatic and polaronic states, ***Journal of Molecular Structure: THEOCHEM*****, 726:** 271-276.
83. A. D. French, A. M. Kelterer, G. P. Johnson, M. K. Dowd, (2000) B3LYP/6-31G*, RHF/6-31G* and MM3 heats of formation of disaccharide analogs, ***Journal of Molecular Structure*****, 556:** 303-313.
84. S. Neihsial, R. H. D. Lyngdoh, (2007) Novel H-bonded base pairs as potential repeat units for information-bearing macromolecular duplexes: A B3LYP/6-31G* search, **Journal *Journal of Molecular Structure: THEOCHEM*****, 806:** 213-221.
85. V. Sortur, J. Yenagi, J. Tonannavar, V. B. Jadhav, M. V. Kulkarni, (2008) Vibrational assignments for 7-methyl-4-bromomethylcoumarin, as aided by RHF and B3LYP/6-31G* calculations, ***Spectrochimica Acta A: Molecular and Biomolecular Spectroscopy*****, 71:** 688-694.
86. P. S. V. Kumar, V. Raghavendra, V. Subramanian, (2016) Bader's theory of atoms in molecules (AIM) and its applications to chemical bonding, ***Journal of Chemical Science*****, 128:** 1527-1536.